

Proportional-Integral-Derivative Gain-Scheduling Control of a Magnetic Levitation System

C.-A. Bojan-Dragos, R.-E. Precup, M.L. Tomescu,
S. Preitl, O.-M. Tanasoiu, S. Hergane

**Claudia-Adina Bojan-Dragos, Radu-Emil Precup,
Stefan Preitl, Oana-Maria Tanasoiu, Stefania Hergane**

Politehnica University of Timisoara
Department of Automation and Applied Informatics
Bd. V. Parvan 2, 300223 Timisoara, Romania
claudia.dragos@aut.upt.ro, radu.precup@upt.ro, stefan.preitl@upt.ro,
oanatanasoiu96@gmail.com, stefania.hergane@yahoo.com

Marius L. Tomescu*

Aurel Vlaicu University of Arad
Romania, 310330 Arad, Elena Dragoi, 2
*Corresponding author: tom_uav@yahoo.com

Abstract: The paper presents a gain-scheduling control design procedure for classical Proportional-Integral-Derivative controllers (PID-GS-C) for positioning system. The method is applied to a Magnetic Levitation System with Two Electromagnets (MLS2EM) laboratory equipment, which allows several experimental verifications of the proposed solution. The nonlinear model of MLS2EM is linearized at seven operating points. A state feedback control structure is first designed to stabilize the process. PID control and PID-GS-C structures are next designed to ensure zero steady-state control error and bumpless switching between PID controllers for the linearized models. Real-time experimental results are presented for validation.

Keywords: gain-scheduling, magnetic levitation system, Proportional-Integral-Derivative control; real-time experiments.

1 Introduction

During the last years several classical and adaptive control structures have been proposed for positioning control system and applications for magnetic levitation systems. Some of these structures are presented in [49], [52], [1], [35], [47], [56], [11], [27], [23], [19], [55], [5]. For example, a high gain adaptive output feedback controller is designed in [5] by introducing two different virtual filters and using back-stepping. Another adaptive control scheme that copes with the modifications of the structural parameters of magnetic levitation systems is suggested in [1].

Gain-scheduling control solutions are popular nowadays, and they are briefly analyzed as follows: fuzzy-based gain scheduling of exact feed-forward linearization control and sliding mode controllers for magnetic ball levitation system are proposed in [28]. A high gain adaptive output feedback control to a magnetic levitation system is discussed in [29]. A Proportional-Integral-Derivative (PID) gain-scheduling controller for second order linear parameter varying, which exclude time varying delay using a Smith predictor is given in [44]. Other interesting adaptive gain scheduling control techniques for real practical applications are given in [6], [54], [7], [17], [53].

The paper is dealing with the position control of a ferromagnetic sphere in a Magnetic Levitation System with Two Electromagnets (MLS2EM) laboratory equipment. A state feedback control structure (SFCS) is first designed in order to stabilize the system by applying the control signal only to the top electromagnet [8]. The simulated external disturbance can be applied

to the bottom electromagnet. Starting with [9] the SFCS is next controlled by a Proportional-Integral-Derivative Gain-Scheduling Control (PID-GS-C) structure. In the presented scheme, the proportional, derivative and integral gains are adapted to the modifications of the operating points. The paper proposes relatively simple classical and adaptive control structures which belongs to the general case of linear and nonlinear control system structures [43], [38], [50], [20], [42], [51], [32], [18], [36].

The paper is organized as follows: the nonlinear model and the linearized mathematical model (MM) of MLS2EM are given in Section 2. The proposed control structure is next developed in Section 3. The real-time experimental results are presented in Section 4 and the conclusions are highlighted in Section 5.

2 Process modeling

The controlled MLS2EM laboratory equipment includes: two electromagnets (EM1 - the top electromagnet and EM2 - the bottom electromagnet), the ferromagnetic sphere, sensors to detect position of the sphere, computer interface, drivers, power supply unit, connection cables and an acquisition board. The nonlinear state-space MM of ML2SEM is [24]:

$$\begin{aligned} \dot{p}(t) &= v(t), \\ \dot{v}(t) &= -\frac{i_{EM1}^2(t) \cdot F_{emP1} \cdot \exp(-p(t)/F_{emP2})}{m \cdot F_{emP2}} + g + \frac{i_{EM2}^2(t) \cdot F_{emP1} \cdot \exp(-(x_d - p(t))/F_{emP2})}{m \cdot F_{emP2}}, \\ \dot{i}_{EM1}(t) &= \frac{k_i \cdot u_{EM1}(t) + c_i - i_{EM1}(t)}{\frac{f_{iP1}}{f_{iP2}} \cdot \exp(-p(t)/f_{iP2})}, \\ \dot{i}_{EM2}(t) &= \frac{k_i \cdot u_{EM2}(t) + c_i - i_{EM2}(t)}{\frac{f_{iP1}}{f_{iP2}} \cdot \exp(-(x_d - p(t))/f_{iP2})}, \\ y(t) &= k_m \cdot p(t), \end{aligned} \quad (1)$$

where: $p \in [0, 0.0016]$ - the sphere position (m), $v \in \mathfrak{R}$ - the sphere speed (m/s), $i_{EM1}, i_{EM2} \in [0.03884, 2.38]$ - the currents in the top electromagnet (EM1) and bottom electromagnet (EM2) (A), $u_{EM1}, u_{EM2} \in [0.005, 1]$ - the signals applied to EM1 and EM2, respectively (V), and y - the process output (m), i.e., the measured sphere position. The parameters of the process are determined analytically and experimentally [24], [16].

The model (1) is linearized around seven operating points (o.p.s) with the coordinates $P^{(j)}(p^{(j)}, v^{(j)}, i_{EM1}^{(j)}, i_{EM2}^{(j)})$ where j is the index of the current operating point, $j = 1 \dots 7$. The linearized state-space models and their matrices are:

$$\begin{aligned} \Delta \dot{\mathbf{x}}^{(j)} &= \mathbf{A}^{(j)} \Delta \mathbf{x}^{(j)} + \mathbf{b}^{(j)} \Delta \mathbf{u}^{(j)}, \\ \Delta y^{(j)} &= \mathbf{c}^{T(j)} \Delta \mathbf{x}^{(j)}, \\ \Delta \mathbf{x}^{(j)} &= [\Delta p^{(j)} \ \Delta v^{(j)} \ \Delta i_{EM1}^{(j)} \ \Delta i_{EM2}^{(j)}]^T, \quad \Delta \mathbf{u}^{(j)} = [\Delta u_{EM1}^{(j)} \ \Delta u_{EM2}^{(j)}]^T, \\ \mathbf{A}^{(j)} &= \begin{bmatrix} 0 & 1 & 0 & 0 \\ a_{21}^{(j)} & 0 & a_{23}^{(j)} & a_{24}^{(j)} \\ a_{31}^{(j)} & 0 & a_{33} & 0 \\ a_{41}^{(j)} & 0 & 0 & a_{44}^{(j)} \end{bmatrix}, \mathbf{b}^{(j)} = [\mathbf{b}_{u_{EM1}}^{(j)} \ \mathbf{b}_{u_{EM2}}^{(j)}] = \begin{bmatrix} 0 & 0 \\ 0 & 0 \\ b_{31}^{(j)} & 0 \\ 0 & b_{42}^{(j)} \end{bmatrix}, \mathbf{c}^{T(j)} = [1 \ 0 \ 0 \ 0], \end{aligned} \quad (2)$$

where T stands for matrix transposition, with the following elements of the matrices $\mathbf{A}^{(j)}$ and $\mathbf{b}^{(j)}$, which depend on $P^{(j)}$:

$$\begin{aligned}
 a_{21}^{(j)} &= \frac{i_{EM1}^{(j)2}}{m} \frac{F_{emP1}}{F_{emP2}^2} \exp(-p^{(j)}/F_{emP2}) + \frac{i_{EM2}^{(j)2}}{m} \frac{F_{emP1}}{F_{emP2}^2} \exp(-(x_d - p^{(j)})/F_{emP2}), \\
 a_{23}^{(j)} &= -\frac{2i_{EM1}^{(j)}}{m} \frac{F_{emP1}}{F_{emP2}} \exp(-p^{(j)}/F_{emP2}), \quad a_{24}^{(j)} = \frac{2i_{EM2}^{(j)}}{m} \frac{F_{emP1}}{F_{emP2}} \exp(-(x_d - p^{(j)})/F_{emP2}), \\
 a_{31}^{(j)} &= -(k_i u_{EM1}^{(j)} + c_i - i_{EM1}^{(j)}) \frac{p^{(j)}}{f_{iP1}} \exp(p^{(j)}/f_{iP2}), \quad a_{33}^{(j)} = -\frac{f_{iP2}}{f_{iP1}} \cdot e^{\frac{x_{10}}{f_{iP2}}}, \\
 a_{41}^{(j)} &= -(k_i u_{EM2}^{(j)} + c_i - i_{EM2}^{(j)}) \frac{p^{(j)}}{f_{iP1}} \exp((x_d - p^{(j)})/f_{iP2}), \quad a_{44}^{(j)} = -\frac{f_{iP2}}{f_{iP1}} \exp((x_d - p^{(j)})/f_{iP2}), \\
 b_{31}^{(j)} &= k_i \frac{f_{iP2}}{f_{iP1}} \exp(p^{(j)}/f_{iP2}), \quad b_{42}^{(j)} = k_i \frac{f_{iP2}}{f_{iP1}} \exp((x_d - p^{(j)})/f_{iP2}).
 \end{aligned} \tag{3}$$

The operating points were chosen as follows such that to belong to the steady-state zone of the sphere position sensor input-output map [33], to cover the usual operating regimes and to avoid the extremities of the input-output map due to instability that may occur:

$$\begin{aligned}
 &P^{(1)}(0.0063, 0, 1.22, 0.39), P^{(2)}(0.007, 0, 1.145, 0.39), P^{(3)}(0.0077, 0, 1.07, 0.39), \\
 &P^{(4)}(0.0084, 0, 1, 0.39), P^{(5)}(0.009, 0, 0.9345, 0.39), P^{(6)}(0.0098, 0, 0.89, 0.39), \\
 &P^{(7)}(0.0105, 0, 0.83, 0.39).
 \end{aligned} \tag{4}$$

The transfer function (t.f) of the state-space linearized MM (2) used in the control system design is:

$$H_{PC}^{(j)}(s) = \mathbf{c}^T(s\mathbf{I} - \mathbf{A}^{(j)})^{-1} \mathbf{b}_{u_{EM1}}^{(j)} = \frac{k^{(j)}}{\prod_{k=1}^3 (s - p_k^{(j)})} = \frac{k_p^{(j)}}{\prod_{k=1}^3 (1 + T_k^{(j)} s)}, \tag{5}$$

where $k_p^{(j)} = k^{(j)} / \prod_{k=1}^3 p_k^{(j)}$, \mathbf{I} is the third-order identity matrix and the time constants are $T_k^{(j)} = -1/p_k^{(j)}$, $k = 1...3$, $j = 1...7$. The expressions of the t.f.s $H_{PC}^{(j)}(s)$ are given in [22], [23].

3 Control solutions design

In order to support the development of next control solutions, the SFCS is designed for the reduced third-order linear mathematical model ($u_2 = u_{EM2} = 0$) of unstable magnetic levitation system [22]. The first three state variables are kept and they lead to the state vector $\mathbf{x} = [p \ v \ i_{EM1}]^T$.

The pole placement method is applied to compute the state feedback gain matrix, $\mathbf{k}_c^{T(j)} = [k_{c1}^{(j)} \ k_{c2}^{(j)} \ k_{c3}^{(j)}]^T$, $j = 1...7$. Therefore, for each linearized MM, with the t.f. $H_{PC}^{(j)}(s)$ (5), the closed-loop system poles $p_k^{*(j)}$, $k = 1...3$, $j = 1...7$, [22], [23], have been imposed in order to guarantee the stability of the linearized system. With the obtained state feedback gain matrix, $\mathbf{k}_{cbest}^T = \mathbf{k}_c^T_{-5} = [66.63 \ 1.62 \ -0.15]$, two types of closed-loop t.f.s of the new state feedback control structure (nSFCS), $H_{SFCS_5}^{(j)}(s)$ result as:

$$\begin{aligned}
 H_{SFCS_5}^{(j)}(s) &= H_x^{(j)}(s) = \mathbf{c}^T(s\mathbf{I} - \mathbf{A}_{x_5}^{(j)})^{-1} \mathbf{b}_{u_{EM1}}^{(j)} = \mathbf{c}^T(s\mathbf{I} - (\mathbf{A}^{(j)} - \mathbf{b}_{u_{EM1}}^{(j)} \mathbf{k}_c^T_{-5} k_{AS}))^{-1} \mathbf{b}_{u_{EM1}}^{(j)} \\
 &= \begin{cases} \frac{k_{SFCS_5}^{(j)}}{(1+T_{1x_5}^{(j)}s)(1+2c_5^{(j)}T_{2x_5}^{(j)}s+T_{2x_5}^{(j)2}s^2)}, & j = 1...3, j \in \{6, 7\}, \\ \frac{k_{SFCS_5}^{(j)}}{(1+T_{1x_5}^{(j)}s)(1+T_{2x_5}^{(j)}s)(1+T_{3x_5}^{(j)}s)}, & j \in \{4, 5\}. \end{cases}
 \end{aligned} \tag{6}$$

Table 1: nSFCS poles and parameters

O.p.	nSFCS poles			nSFCS parameters				
	$p_{1_5}^{*(j)}$	$p_{2_5}^{*(j)}$	$p_{3_5}^{*(j)}$	$k_{SFCS_5}^{(j)}$	$T_{1x_5}^{(j)}$	$T_{2x_5}^{(j)}$	$\zeta_5^{(j)}$	$T_{etax_5}^{(j)}$
(1)	-0.79+1.02i	-0.79-1.02i	-0.10	0.084	0.0988	-	0.6	0.0077
(2)	-0.92+0.88i	-0.92-0.88i	-0.13	0.065	0.0778	-	0.7	0.0078
(3)	-1.07+0.62i	-1.07-0.62i	-0.16	0.054	0.0618	-	0.9	0.0081
(4)	-1.65	-0.82	-0.21	0.046	0.0485	0.0123	-	-
(5)	-2.32	-0.41	-0.32	0.041	0.0314	0.0244	-	-
(6)	-3.07	-0.28+0.16i	-0.28-0.16i	0.038	0.0033	-	0.9	0.0308
(7)	-3.78	-0.23+0.20i	-0.23-0.20i	0.034	0.0026	-	0.7	0.0332

The new SFCS poles obtained with the state feedback gain matrix $\mathbf{k}_{c_5}^T$ and the nSFCS parameters used next in the PID-GS-C structure are given in Table 1.

Due to the fact that the natural SFCS does not contain an I component, so it cannot ensure the zero steady-state control error, the SFCS, as controlled plant, is included in a cascade control structure (CCS) with PID controller in the outer loop. Depending on the operating points, seven control solutions with PID controllers have been designed using pole-zero cancellation. The t.f.s of the designed PID controllers extended with a first order lag filter can be expressed as:

$$H_{PID_5}^{(j)}(s) = \begin{cases} \frac{k_{c_5}^{(j)}(1+2\zeta_{c_5}^{(j)}T_{c_5}^{(j)}s+T_{c_5}^{(j)2}s^2)}{s(1+T_{fd_5}^{(j)}s)}, & j \in \{1, 2, 3, 6, 7\}, \\ \frac{k_{c_5}^{(j)}(1+T_{c1_5}^{(j)}s)(1+T_{c2_5}^{(j)}s)}{s(1+T_{fd_5}^{(j)}s)}, & j \in \{4, 5\}, \end{cases} \quad (7)$$

with the tuning parameters $k_{c_5}^{(j)}$, $T_{c_5}^{(j)}$, $T_{c1_5}^{(j)}$, $T_{c2_5}^{(j)}$ and $T_{fd_5}^{(j)}$:

$$k_{c_5}^{(j)} = \begin{cases} 1/(2 \cdot k_{SFCS_5}^{(j)} \cdot T_{etax_5}^{(j)}), & j = 1...3 \\ 0.05/(2 \cdot k_{SFCS_5}^{(j)} \cdot T_{\Sigma x_5}^{(j)}), & j \in \{4, 5\} \\ 0.01/(2 \cdot k_{SFCS_5}^{(j)} \cdot T_{1x_5}^{(j)}), & j \in \{6, 7\}, \end{cases} \quad (8)$$

$$\begin{cases} T_{c_5}^{(j)} = T_{etax_5}^{(j)}, & j \in \{1, 2, 3, 6, 7\}, \\ T_{c1_5}^{(j)} = T_{1x_5}^{(j)}, & j \in \{4, 5\}, \\ T_{c2_5}^{(j)} = T_{2x_5}^{(j)}, & j \in \{4, 5\}, \\ T_{fd_5}^{(j)} = 0.1 \cdot T_{1x_5}^{(j)}, & j = 1...7, \end{cases} \quad \zeta_{c_5}^{(j)} = \zeta_5^{(j)}.$$

Due to the oscillatory regime, the t.f.s coefficients $k_{c_5}^{(j)}$ must be adjusted. The numerical values of PID-C parameters and the system performance indices – overshoot and settling time – are synthesized in Table 2.

Due to the process nonlinearities, which also depend on the operating point, the switching from one PID controller to another one is a useful solution to ensure improved performance according to [48]. Therefore, a PID-GS-C structure illustrated in Figure 1 is designed. The PID-GS-C structure is developed on the basis of the PID controller (with the notation PID-C in Figure 1), with the t.f.:

$$\Delta u_{1x}(t) = k_p(t)e(t) + k_i(t) \int e(t)dt + k_d(t)\dot{e}(t), \quad (9)$$

where k_p is the proportional gain, k_d is the derivative gain and k_i is the integral gain.

Table 2: PID controller parameters

O.p.	PID controller tuning parameters		PID control system performance indices	
	$k_c^{(j)}$	$T_c^{(j)}$	$t_r^{(j)}$	$\sigma_1^{(j)}$
(1)	60.65	0.009	4,25	0,24
(2)	98.23	0.008	4,25	0,24
(3)	150.83	0.006	4,5	0,24
(4)	89.88	0.005	5,0	0,23
(5)	28.67	0.003	4,0	0,23
(6)	40.98	0.003	3,5	0,24
(7)	111.24	0.003	4,0	0,24

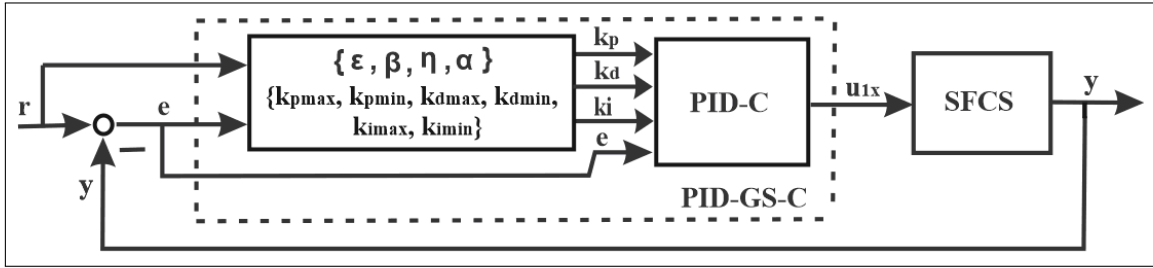


Figure 1: Block diagram of PID-GS-C system structure

As shown in Figure 1, the gain-scheduling (GS) block uses the reference input $r(t)$ and the control error $e(t)$ as input variables, and the tuning parameters of the PID-C, namely k_p , k_d and k_i , as output variables. The PID tuning parameters are obtained as follows:

$$\begin{aligned}
 k_p(t) &= k_{p \max} - (k_{p \max} - k_{p \min}) \exp[-(\alpha(t)|e(t)|)], \\
 k_d(t) &= k_{d \max} - (k_{d \max} - k_{d \min}) \exp[-(\alpha(t)|e(t)|)], \\
 k_i(t) &= (1 - \alpha(t))k_{i \max}.
 \end{aligned} \tag{10}$$

The parameters $k_{p \max}$, $k_{p \min}$, $k_{d \max}$, $k_{d \min}$, $k_{i \max}$ and $k_{i \min}$ are determined from the PID-GS-C tuning parameters:

$$\begin{aligned}
 k_{p \max} &= \begin{cases} \max[k_c^{(j)} \cdot (T_{c1}^{(j)} + T_{c2}^{(j)})], j \in \{4, 5\}, \\ \max[2 \cdot k_c^{(j)} \cdot \zeta_c^{(j)} \cdot T_c^{(j)}], j \in \{1, 2, 3, 6, 7\}, \end{cases} \\
 k_{p \min} &= \begin{cases} \min[k_c^{(j)} \cdot (T_{c1}^{(j)} + T_{c2}^{(j)})], j \in \{4, 5\}, \\ \min[2 \cdot k_c^{(j)} \cdot \zeta_c^{(j)} \cdot T_c^{(j)}], j \in \{1, 2, 3, 6, 7\}, \end{cases} \\
 k_{d \max} &= \begin{cases} \max(k_c^{(j)} \cdot T_{c1}^{(j)} \cdot T_{c2}^{(j)}), j \in \{4, 5\}, \\ \max(k_c^{(j)} \cdot T_c^{(j)^2}), j \in \{1, 2, 3, 6, 7\}, \end{cases} \\
 k_{d \min} &= \begin{cases} \min(k_c^{(j)} \cdot T_{c1}^{(j)} \cdot T_{c2}^{(j)}), j \in \{4, 5\}, \\ \min(k_c^{(j)} \cdot T_c^{(j)^2}), j \in \{1, 2, 3, 6, 7\}, \end{cases} \\
 k_{i \max} &= \max(k_c^{(j)}), k_{i \min} = \min(k_c^{(j)}), j = 1 \dots 7.
 \end{aligned} \tag{11}$$

The parameter $0 \leq \alpha(t) \leq 1$ is included in order to have a smooth and continuous variation of the switching from one PID controller to another one. The following equation is used to get the value of this parameter:

$$\alpha(t) = \tanh(\eta\beta(t)) = [\exp(2\eta\beta(t)) - 1]/[\exp(2\eta\beta(t)) + 1], \tag{12}$$

where the parameter η determines the rate at which $\alpha(t)$ changes between 0 and 1 and chosen in order to ensure a certain dynamics of the variation of $\alpha(t)$. The parameter $\beta(t)$ is set in terms of [35]:

$$\beta(t) = \begin{cases} 1, & |e(t)| > \xi, \\ 0, & |e(t)| < \xi, \end{cases}, \quad \xi = 0.9 \cdot r(t). \quad (13)$$

As shown in [35], to design the PID-GS-C structure, the following conditions can be taken into account: when the system is in steady-state error (i.e., $|e(t)|$ is large), $k_{p\max}$ and $k_{i\min}$ are activated in order to produce a large control signal and to overcome the undesirable oscillation and overshoot; during the steady-state regime, $k_{i\max}$ and $k_{p\min}$ are activated to obtain a small value of $|e(t)|$ and to overcome the undesirable problem of overshoot.

4 Experimental results

All control structures, namely, SFCS, PID-C and PID-GS-C, were tested on the nonlinear laboratory system and validated by real-time experiments. In all cases, the reference input was set to 0.007 m from the top electromagnet and the control structures responses were tested on the time frame of 20 s. The responses of the sphere position, the current and the control signal in the top electromagnet were plotted.

The values of the parameters of the PID-GS-C block in Figure 1 are $k_{p\max} = 5516$, $k_{p\min} = 0.6$, $k_{d\max} = 0.1225$, $k_{d\min} = 0.0036$, $k_{i\max} = 151$, $k_{i\min} = 0$ and $\eta \in \{0.001, 0.1\}$. They have been obtained using several experiments such that to get the best values in the context of a compromise to tradeoff to overshoot. But other empirical performance indices can be considered in this tuning.

The following experimental scenarios were considered and performed:

(a) The state feedback control system structure with the best state feedback gain matrix was tested on the laboratory equipment and the results are presented in Figure 2.

(b) The PID controller designed at seven operating points was tested on laboratory equipment. The experimental results of the control system with PID controller designed only for three o.p.s defined in Tables 1 and 2, i.e., (1), (5) and (7) are presented as responses of several variables measured in the laboratory setup in Figures 3 to 5 as follows: the control signal versus time in Figure 3, the current through EM1 versus time in Figure 4 and the controlled output versus time in Figure 5. These results are better in comparison with the results presented in Figure 2 because of the PID-C, which ensures the zero steady-state control error and the reference input is tracked. The pair of complex conjugated poles from the cases that correspond to the o.p.s (1) to (3) (similarly to the o.p.s (6) and (7)) and the nonlinearities of the process lead to oscillations at the beginning of transient responses and during the real-time experiments.

(c) The experimental results of the control system with PID-GS controller are presented as responses of several variables measured in the laboratory setup in Figures 6 to 8 as follows: the control signal versus time in Figure 6, the current through EM1 versus time in Figure 7 and the controlled output versus time in Figure 8. These results are better in comparison with the results presented in Figures 3 to 5 because of the PID-GS controller that ensures improved dynamic behavior characterized by smaller overshoot and settling time.

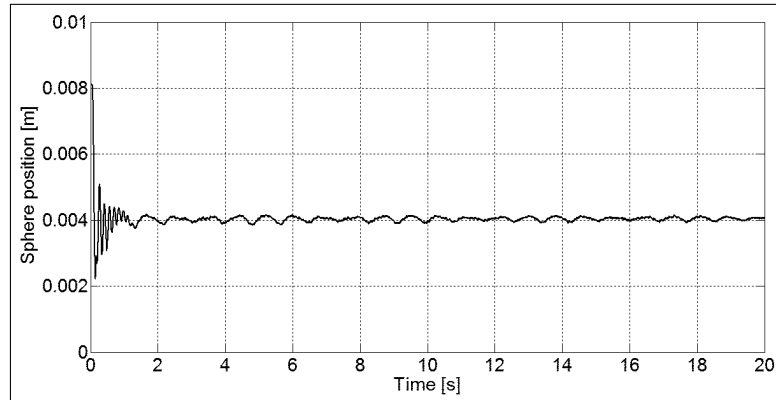


Figure 2: Real-time experimental results of state feedback control system structure with the best state feedback gain matrix

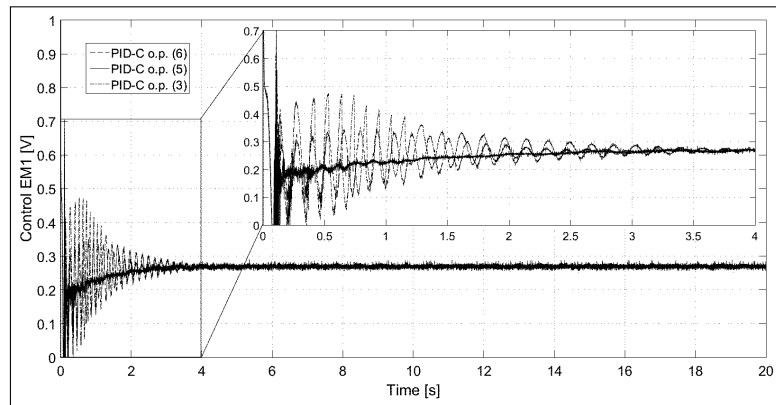


Figure 3: Control signal $u_1 = u_{EM1}^{(j)}$, $j \in \{3, 5, 6\}$, versus time for control systems with PID controller for o.p.s. (3), (5) and (6)

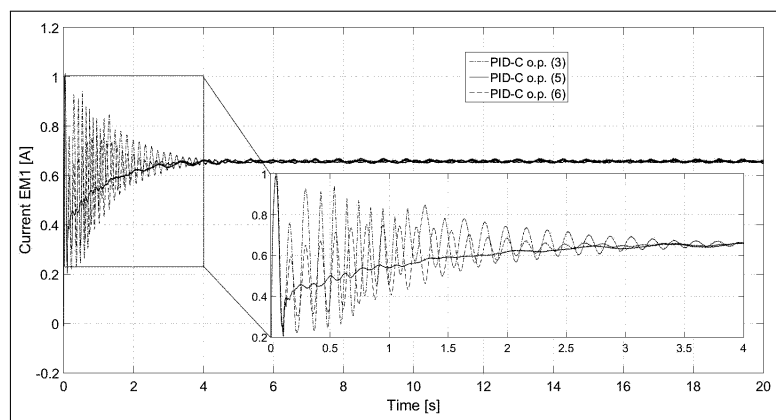


Figure 4: Current i_{EM1} versus time for control systems with PID controller designed for o.p.s. (3), (5) and (6)

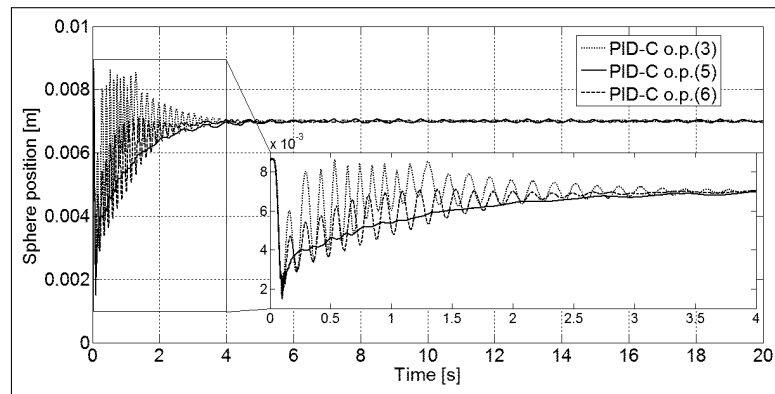


Figure 5: Sphere position p versus time for control systems with PID controller designed for o.p.s. (3), (5) and (6)

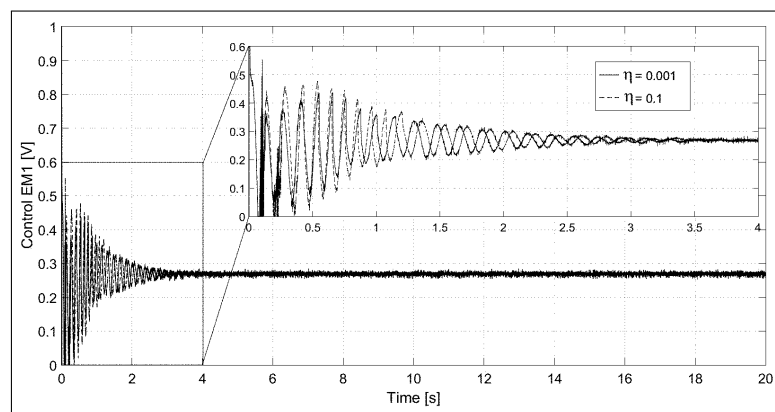


Figure 6: Control signal $u_1 = u_{EM1}^{(j)}$ versus time for control systems with PID-GS controller

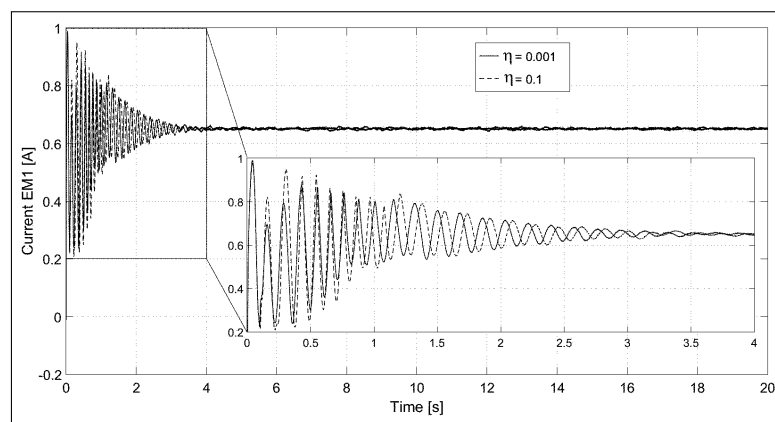


Figure 7: Current i_{EM1} versus time for control systems with PID-GS controller

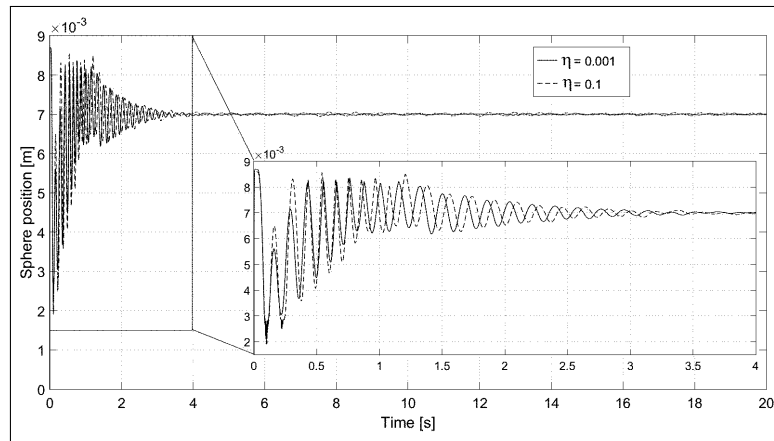


Figure 8: Sphere position p versus time for control systems with PID-GS controller

5 Conclusions

The paper has presented three control structures developed to control the position of the sphere in an MLS2EM laboratory setup. In order to use relatively simple control structures, the presented nonlinear model of the MLS2EM was linearized around seven operating points. To stabilize the process, a state feedback control structures was designed and the best state feedback gain matrix was found.

Since the SFCS does not ensure the zero steady-state control error, seven PID controllers were designed. To ensure the switching between different PID controllers, a PID-GS controller was developed and implemented. All control system structures were tested on the nonlinear model, accepting the main values of the parameters given in [24]. This paper has considered a low-cost implementation of the controllers but this must be viewed in connection with the complexity of the control algorithms, and several approaches can be used [10], [12], [37], [13], [15], [31], [46].

The real-time experimental results prove that the PID-GS-C structure discussed in this paper guarantees the improvement of control system performance regarding to step modifications of reference input. They ensure zero steady-state control error, small overshoot and settling time. As shown in the previous section, the choice of the parameters of the PID-GS-C block in Figure 1 has been carried out by conducting several experiments such that to aim the best values from the point of view of the compromise to the achievement of best overshoot and settling time. This is a limitation of the control system structure presented in this paper.

The systematic choice of the parameters of PID-GS-C will represent a direction of future research by ensuring the optimal tuning using classical [4], [22], [39], [2], [25], [14] and modern optimization algorithms [40], [41], [45], [26], [33], [30], [34], [21], [3] or their combinations. Future research will also be focused on the design of control systems with PI(D) fuzzy gain-scheduling controllers, Takagi-Sugeno fuzzy controllers and hybrid structures including sliding mode control and gain-scheduling control for improved performance indices.

Acknowledgment

This work was supported by grants from the Partnerships in priority areas – PN II program of the Romanian Ministry of National Education and Scientific Research (MENCS) – the Executive Agency for Higher Education, Research, Development and Innovation Funding

(UEFISCDI), project numbers PN-II-PT-PCCA-2013-4-0544, PN-II-PT-PCCA-2013-4-0070 and PN-II-RU-TE-2014-4-0207.

Bibliography

- [1] An S., Ma Y., Cao Z. (2009); Applying simple adaptive control to magnetic levitation system, *Proceedings of 2nd International Conference on Intelligent Computation Technology and Automation*, Changsha, Hunan, China, 1, 746-749, 2009.
- [2] Angelov P., Yager R. (2012); A new type of simplified fuzzy rule-based systems, *International Journal of General Systems*, 41(2), 163-185, 2012.
- [3] Azar D., Fayad K., Daoud C. (2016); A combined ant colony optimization and simulated annealing algorithm to assess stability and fault-proneness of classes based on internal software quality attributes, *International Journal of Artificial Intelligence*, 14(2), 137-156, 2016.
- [4] Baranyi P., Tikk D., Yam Y., Patton R.J. (2003); From differential equations to PDC controller design via numerical transformation, *Computers in Industry*, 51(3), 281-297, 2003.
- [5] Bianchi F.D., Sánchez Peña R.S. (2011); Interpolation for gain-scheduled control with guarantees, *Automatica*, 47(1), 239-243, 2011.
- [6] Bianchi F.D.; Sánchez-Pena R.S., Guadayol M. (2012); Gain scheduled control based on high fidelity local wind turbine models, *Renewable Energy*, 37(1), 233-240, 2012.
- [7] Bedoud K., Ali-rachedi M., Bahid T., Lakel R. (2015); Adaptive fuzzy gain scheduling of PI controller for control of the wind energy conversion systems, *Energy Procedia*, 74, 211-225, 2015.
- [8] Bojan-Dragos C.-A., Preitl S., Precup R.-E., Hergane S., Hughiet E.G., Szedlak-Stinean A.-I. (2016); State feedback and proportional-integral-derivative control of a magnetic levitation system, *Proceedings of IEEE 14th International Symposium on Intelligent Systems and Informatics*, Subotica, Serbia, 111-116, 2016.
- [9] Bojan-Dragos C.-A., Preitl S., Precup R.-E., Hergane S., Hughiet E.G., Szedlak-Stinean A.-I. (2016); Proportional-integral gain-scheduling control of a magnetic levitation system, *Proceedings of 20th International Conference on System Theory, Control and Computing*, Sinaia, Romania, 1-6, 2016.
- [10] Chadli M., Akhenak A., Ragot J., Maquin D. (2009); State and unknown input estimation for discrete time multiple model, *Journal of the Franklin Institute*, 346(6), 593-610, 2009.
- [11] Chauhan S., Nigam M.J. (2014); Model predictive controller design and perturbation study for magnetic levitation system, *Proceedings of 2014 IEEE Recent Advances in Engineering and Computational Sciences*, Chandigarh, India, 1-6, 2014.
- [12] Colhon M., Danciulescu, D. (2010); Semantic schemas for natural language generation in multilingual systems, *Journal of Knowledge, Communications and Computing Technologies*, 2(1), 10-17, 2010.
- [13] Danciulescu D. (2015); Formal languages generation in systems of knowledge representation based on stratified graphs, *Informatica*, 26(3), 407-417, 2015.

-
- [14] Deliparaschos K., Michail K., Zolotas A., Tzafestas S. (2016); FPGA-based efficient hardware/software co-design for industrial systems with systematic sensor selection, *Journal of Electrical Engineering*, 67(3), 150-159, 2016.
 - [15] Derr K.W., Manic M. (2015); Wireless sensor networks - node localization for various industry problems, *IEEE Transactions on Industrial Informatics*, 11(3), 752-762, 2015.
 - [16] Dragos C.-A., Precup R.-E., David R.-C., Preitl S., Stinean A.-I., Petriu E.M. (2013); Simulated annealing-based optimization of fuzzy models for magnetic levitation systems, *Proceedings of 2013 Joint IFSA World Congress and NAFIPS Annual Meeting*, Edmonton, AB, Canada, 286-29, 2013.
 - [17] Dounis A.I., Kofinas P., Alafodimos C., Tseles D. (2013); Adaptive fuzzy gain scheduling PID controller for maximum power point tracking of photovoltaic system, *Renewable Energy*, 60, 202-214, 2013.
 - [18] Dzitac I. (2015); The fuzzification of classical structures: A general view, *International Journal of Computers Communications & Control*, 10(6), 772-788, 2015.
 - [19] Elsodany N.M., Rezeka S.F., Maharem N.A. (2011); Adaptive PID control of a stepper motor driving a flexible rotor, *Alexandria Engineering Journal*, 50(2), 127-136, 2011.
 - [20] Filip F.G. (2008); Decision support and control for large-scale complex systems, *Annual Reviews in Control*, 32(1), 61-70, 2008.
 - [21] Gaxiola F., Melin P., Valdez F., Castro J.R., Castillo O. (2016); Optimization of type-2 fuzzy weights in backpropagation learning for neural networks using GAs and PSO, *Applied Soft Computing*, 38, 860-871, 2016.
 - [22] Haber R.E., Alique J.R. (2007); Fuzzy logic-based torque control system for milling process optimization, *IEEE Transactions on Systems, Man and Cybernetics, Part C: Applications and Reviews*, 37(5), 941-950, 2007.
 - [23] Huang Y.-W., Tung P.-C. (2009); Design of a fuzzy gain scheduling controller having input saturation: a comparative study, *Journal of Marine Science and Technology*, 17(4), 249-256, 2009.
 - [24] Inteco. (2008); Magnetic Levitation System 2EM (MLS2EM), User's Manual (Laboratory Set), Inteco Ltd., Krakow, Poland, 2008.
 - [25] Johanyák Z.C. (2013); Fuzzy modeling of thermoplastic composites' melt volume rate, *Computing and Informatics*, 32(4), 845-857, 2013.
 - [26] Kazakov A.L., Lempert A.A. (2015); On mathematical models for optimization problem of logistics infrastructure, *International Journal of Artificial Intelligence*, 13(1), 200-210, 2010.
 - [27] King R., Stathaki A. (2000); Fuzzy gain scheduling control of nonlinear processes, *Research Report, Department of Electrical and Computer Engineering*, University of Patras, Patras, Greece, 2000.
 - [28] Lashin M., Elgammal A.T., Ramadan A., Abouelsoud A.A., Assal S.F.M., Abo-Ismael A. (2014); Fuzzy-based gain scheduling of exact feedforward linearization control and SMC for magnetic ball levitation system: A comparative study, *Proceedings of 2014 IEEE International Conference on Automation, Quality and Testing, Robotics*, Cluj-Napoca, Romania, 1-6, 2014.

-
- [29] Michino R., Tanaka H., Mizumoto I. (2009); Application of high gain adaptive output feedback control to a magnetic levitation system, *Proceedings of ICROS-SICE International Joint Conference*, Fukuoka, Japan, 970-975, 2009.
- [30] Moharam A., El-Hosseini M.A., Ali H.A. (2015); Design of optimal PID controller using NSGA-II algorithm and level diagram, *Studies in Informatics and Control*, 24(3), 301-308, 2015.
- [31] Negru V., Grigoras G., Danciulescu D. (2015); Natural language agreement in the generation mechanism based on stratified graphs, *Proceedings of 7th Balkan Conference in Informatics*, Craiova, Romania, 36:1-36:8, 2015.
- [32] Obe O., Dumitrache I. (2012); Adaptive neuro-fuzzy controller with genetic training for mobile robot control, *International Journal of Computers Communications & Control*, 7(1), 135-146, 2012.
- [33] Osaba E., Onieva E., Dia F., Carballedo R., Lopez P., Perallos A. (2015); A migration strategy for distributed evolutionary algorithms based on stopping non-promising subpopulations: A case study on routing problems, *International Journal of Artificial Intelligence*, 13(2), 46-56, 2015.
- [34] Osaba E., Yang X.-S., Diaz F., Lopez P., Carballedo R. (2016); An improved discrete bat algorithm for symmetric and asymmetric traveling salesman problems, *Engineering Applications of Artificial Intelligence*, 48, 59-71, 2016.
- [35] Pallav S., Pandey K., Laxmi V. (2014); PID control of magnetic levitation system based on derivative filter, *Proceedings of 2014 Annual International Conference on Emerging Research Areas: Magnetics, Machines and Drives*, Kottayam, India, 1-5, 2014.
- [36] Precup R.-E., Angelov P., Costa B.S.J., Sayed-Mouchaweh M. (2015); An overview on fault diagnosis and nature-inspired optimal control of industrial process applications, *Computers in Industry*, 74, 75-94, 2015.
- [37] Precup R.-E., David R.-C., Petriu E.M., Preitl S., Radac M.-B. (2014); Novel adaptive charged system search algorithm for optimal tuning of fuzzy controllers, *Expert Systems with Applications*, 41(4), 1168-1175, 2014.
- [38] Precup R.-E., Preitl S. (1997); Popov-type stability analysis method for fuzzy control systems, *Proceedings of Fifth European Congress on Intelligent Technologies and Soft Computing*, Aachen, Germany, 2, 1306-1310, 1997.
- [39] Precup R.-E., Preitl S. (2007); PI-fuzzy controllers for integral plants to ensure robust stability, *Information Sciences*, 177(20), 4410-4429, 2007.
- [40] Precup R.-E., Sabau, M.-C., Petriu E.M. (2015); Nature-inspired optimal tuning of input membership functions of Takagi-Sugeno-Kang fuzzy models for anti-lock braking systems, *Applied Soft Computing*, 27, 575-589, 2015.
- [41] Precup R.-E., Radac M.-B., Tomescu M.L., Petriu E.M., Preitl S. (2013); Stable and convergent iterative feedback tuning of fuzzy controllers for discrete-time SISO systems, *Expert Systems with Applications*, 40(1), 188-199, 2013.
- [42] Precup R.-E., Tomescu M.L., Preitl S. (2009); Fuzzy logic control system stability analysis based on Lyapunov's direct method, *International Journal of Computers Communications & Control*, 4(4), 415-426, 2009.

-
- [43] Preitl S., Precup R.-E. (1996); On the algorithmic design of a class of control systems based on providing the symmetry of open-loop Bode plots, *Scientific Bulletin of UPT, Transactions on Automatic Control and Computer Science*, 41(55)(2), 47-55, 1996.
 - [44] Puig V., Bolea Y., Blesa J. (2012); Robust gain-scheduled Smith PID controllers for second order LPV systems with time varying delay, *IFAC Proceedings Volumes*, 45(3), 199-204, 2012.
 - [45] Rebai A., Guesmi K., Hemicci B. (2015); Design of an optimized fractional order fuzzy PID controller for a piezoelectric actuator, *Control Engineering and Applied Informatics*, 17(3), 41-49, 2015.
 - [46] Qin Q., Cheng S., Zhang, Q., Qin Q., Cheng S., Zhang Q., Li L., Shi Y. (2016); Particle swarm optimization with interswarm interactive learning strategy, *IEEE Transactions on Cybernetics*, 46(10), 2238-2251, 2016.
 - [47] Sakalli A., Kumbasar T., Yesil E., Hagraş H. (2014); Analysis of the performances of type-1, self-tuning type-1 and interval type-2 fuzzy PID controllers on the magnetic levitation system, *Proceedings of 2014 IEEE International Conference on Fuzzy Systems*, Beijing, China, 1859-1866, 2014.
 - [48] Sedaghati A. (2006); A PI controller based on gain-scheduling for synchronous generator, *Turkish Journal of Electrical Engineering and Computer Sciences*, 14(2), 241-251, 2006.
 - [49] Shameli E., Khamesee M.B., Huissoon J.P. (2007); Nonlinear controller design for a magnetic levitation device, *Microsystem Technologies*, 13(8), 831-835, 2007.
 - [50] Škrjanc I., Blažič S., Agamennoni O.E. (2005); Interval fuzzy model identification using l_∞ -norm, *IEEE Transactions on Fuzzy Systems*, 13(5), 561-568, 2005.
 - [51] Vaščák J. (2010); Approaches in adaptation of fuzzy cognitive maps for navigation purposes, *Proceedings of 8th International Symposium on Applied Machine Intelligence and Informatics*, Heržany, Slovakia, 31-36, 2010.
 - [52] Wang B.; Liu G.-P.; Rees D. (2009); Networked predictive control of magnetic levitation system, *Proceedings of 2009 IEEE International Conference on Systems, Man and Cybernetics*, San Antonio, TX, USA, 4100-4105, 2009.
 - [53] Xie Y.-M., Shi H., Alleyne A., Yang B.-G. (2016); Feedback shape control for deployable mesh reflectors using gain scheduling method, *Acta Astronautica*, 121, 241-255, 2016.
 - [54] Yang Y.-N., Yan Y. (2016); Attitude regulation for unmanned quadrotors using adaptive fuzzy gain-scheduling sliding mode control, *Aerospace Science and Technology*, 54, 208-217, 2016.
 - [55] Zhao Z.Y., Tomizuka M. (1993); Fuzzy gain scheduling of PID controllers, *IEEE Transactions on Systems, Man, and Cybernetics*, 23(5), 1392-1398, 1993.
 - [56] Zietkiewicz J. (2011); Constrained predictive control of a levitation system, *Proceedings of 16th International Conference on Methods and Models in Automation and Robotics*, Miedzyzdroje, Poland, 278-283, 2011.